

Catalysis Science & Technology

Accepted Manuscript



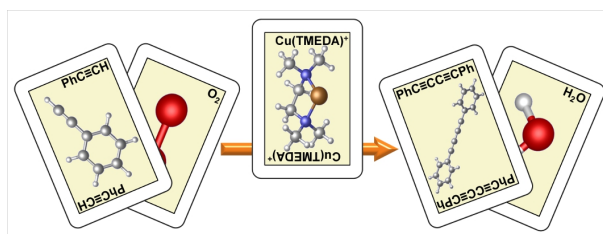
This is an *Accepted Manuscript*, which has been through the Royal Society of Chemistry peer review process and has been accepted for publication.

Accepted Manuscripts are published online shortly after acceptance, before technical editing, formatting and proof reading. Using this free service, authors can make their results available to the community, in citable form, before we publish the edited article. We will replace this *Accepted Manuscript* with the edited and formatted *Advance Article* as soon as it is available.

You can find more information about *Accepted Manuscripts* in the [Information for Authors](#).

Please note that technical editing may introduce minor changes to the text and/or graphics, which may alter content. The journal's standard [Terms & Conditions](#) and the [Ethical guidelines](#) still apply. In no event shall the Royal Society of Chemistry be held responsible for any errors or omissions in this *Accepted Manuscript* or any consequences arising from the use of any information it contains.

Graphical abstract



The full reaction mechanism for the copper catalyzed oxidative coupling of two terminal alkynes is computationally characterized with DFT methods

Cite this: DOI: 10.1039/c0xx00000x

www.rsc.org/xxxxxx

ARTICLE TYPE

Toward a mechanistic understanding of oxidative homocoupling: the Glaser–Hay reaction

Jesús Jover,^a Philipp Spuhler,^b Ligang Zhao,^b Ciarán McArdle^b and Feliu Maseras^{*a,c}

Received (in XXX, XXX) Xth XXXXXXXXXX 20XX, Accepted Xth XXXXXXXXXX 20XX

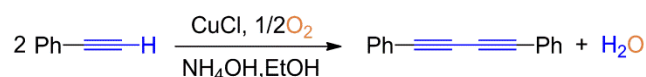
DOI: 10.1039/b000000x

The copper-catalyzed oxidative homocoupling of terminal alkynes has been studied with DFT methods. The role of Cu(I) or Cu(II) as initial oxidation state, as well as the effect of changes in the substrate and the base have been examined. Oxidants responsible for outer- and inner-sphere electron transfer processes have been also investigated. The Cu/O₂ interactions, which arise when dioxygen is employed as oxidant, have been treated explicitly to fully describe the 4-electron reduction process, providing a plausible mechanism that could serve as a model for other aerobic oxidative couplings. The obtained results completely agree with the reported experimental data, the computed free energy barriers are low enough for the reactions to proceed at room temperature, and electron-poor alkynes and stronger bases lead to faster reactions.

15 Introduction

Metal-mediated coupling reactions have become one of the main tools to carry out the formation of C–C bonds.¹ The importance of cross-coupling, between an R–X (X= halide) and R'–Y (Y=electropositive group) was recognized by Nobel Prize in 2010.² Not all systems are however amenable to cross-coupling, and as a result, homocoupling, where the reaction occurs between two identical partners, is also a subject of interest. In homocoupling, an external reducing or oxidating³ agent is often necessary to bring the metal back to its initial oxidation state. The use of dioxygen in oxidative homocoupling is particularly appealing because only water is formed as byproduct of the oxidation.⁴

One of the earliest and most simple examples of oxidative homocoupling is the Glaser reaction, reported originally in 1869.⁵ Glaser observed that a mixture of phenylacetylene, copper (I) chloride and ammonium hydroxide in ethanol, when exposed to air, smoothly formed diphenyldiacetylene (Scheme 1). The scope of the reaction was later expanded, as it was stated that O₂ can be replaced by many other oxidants.^{6,7} A crucial modification of the reaction, reported by Hay in the 1960s,⁸ indicated that the addition of nitrogen ligands such as TMEDA (N,N,N',N'-tetramethylethylenediamine) allowed the reaction to be carried out under mild conditions using copper (I) chloride as catalyst. Since then a variety of copper (I) and (II) salts and nitrogen ligands, i.e. tertiary amines or pyridines, have been used to perform the oxidative coupling of acetylenes providing good results.^{9,10-12} In most experiments, a ligand excess or an external base is added because it has been demonstrated that the reaction is faster under basic conditions. Different bases, ranging from the ammonium hydroxide employed by Glaser to organic amines¹¹⁻¹³ (e.g. piperidine, NEt₃, etc) or inorganic salts such as sodium



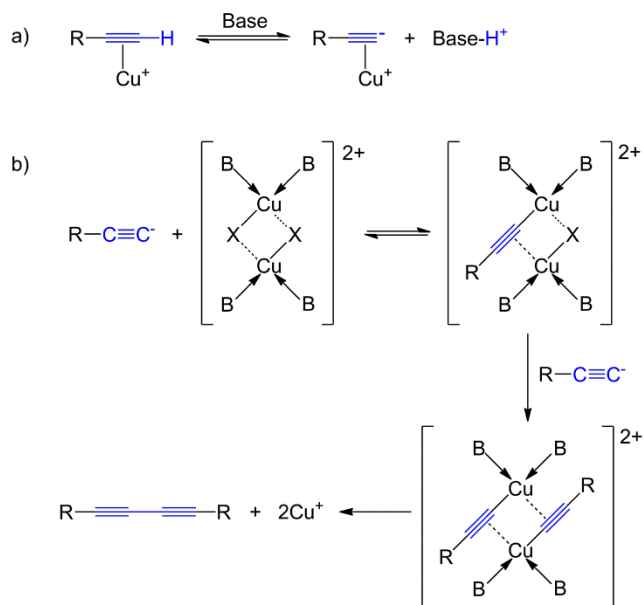
Scheme 1 Oxidative coupling of phenylacetylene as described by Glaser.

carbonate or acetate have been employed.^{14,15} Another piece of relevant experimental information states that acidic acetylenes produce the fastest reaction rates,¹⁶ indicating that the terminal proton abstraction plays a crucial role on the mechanism.

The Glaser–Hay reaction is technologically relevant, as the 1,3-diyne products obtained have a wide range of interesting applications in optical materials, organic conductors and molecular devices¹⁷ as well as antifungal activity,¹⁸ conducting polymers and liquid crystals.¹⁹ On the other hand, the study of simple Glaser coupling reactions can serve as a benchmark for other, more complicated, oxidative coupling reactions where dioxygen is employed as oxidant. Even more, improving our knowledge of these reactions can be used to better understand more complicated systems such as copper oxydases²⁰ and oxygenases²¹ e.g. superoxide dismutase or tyrosinase, or even oxygen evolution systems.²²

The detailed mechanism of the Glaser–Hay reaction remains to be determined. One of the most elaborate proposals was made by Bohlmann and co-workers in 1964,¹⁶ summarized in Scheme 2. According to their scheme, the reaction starts with the π -coordination of the triple bond to a copper (I) species that facilitates the activation of the terminal C–H bond by an external base. It was also proposed that the 1,3-diyne is formed by reductive elimination from a dinuclear copper (II) acetylide species (Scheme 2b). The Bohlmann mechanism neglects however the crucial oxidation step required to close the cycle, as part b) starts with copper (II) but ends up with copper (I).

An alternative proposal was made more recently based on B3LYP DFT calculations.²³ A lot of emphasis was placed in this



Scheme 2 Bohlmann proposal for Glaser coupling of acetylenes (B = N ligand).

case in the interaction between copper and dioxygen, but the results had serious shortcomings. A detailed analysis of the computed thermodynamics reveals that the although the reported potential energy barrier for the catalytic cycle is around 22 kcal/mol, the value increases above 50 kcal/mol when free energy corrections are introduced. In addition, the proposed mechanism is completely specific for the employed reactants and it cannot explain why the reaction proceeds with different copper sources and oxidants. The appropriateness of the B3LYP functional for the description of Cu_2O_2 cores has been also called into question.^{24,25} Some critical aspects of the reaction remain insufficiently explained in these proposals. In particular, a full mechanism must explain why the reaction seems to operate similarly regardless of the oxidant used. This is particularly shocking because of the use of one-electron oxidants, such as $\text{K}_3[\text{Fe}(\text{CN})_6]$, and two- or four-electron oxidants, such as dioxygen. The mechanism must also explain why the reaction is faster under basic conditions¹⁰⁻¹⁴ and when acidic acetylenes are used.¹⁶ The role of dioxygen is particularly intriguing, as despite the increased interest in the use of this oxidant in systems involving copper, little is known about its detailed reaction mechanism.^{12,15,25-29} Computational studies in the role of copper oxygen systems in homogeneous catalysis are scarce and focused on very specific cases.^{23,30}

We present in this article a computational study on the mechanism of the Glaser–Hay reaction. Computational applications to aerobic oxidative coupling have been limited,²³ but they have a long story of success in cross-coupling³¹ and other processes involving electron transfer in copper complexes.³² As a first approach, a general mechanism, valid for most outer sphere oxidants along with copper (I) reagents will be studied. At this stage $\text{K}_3[\text{Fe}(\text{CN})_6]$ will be employed as the benchmark oxidant, representative of those that can be found in the literature. Then, the mechanism of the catalytic reaction starting from copper (II) will be evaluated with the same kind of oxidants. Afterwards, the full Glaser–Hay reaction mechanism will be

studied to model the explicit interaction between the metal species and O_2 when the latter is used as oxidant; this will show how the dioxygen works in aerobic oxidative copper-coupling catalyzed reactions.

45 Computational Methods

All the structures have been fully optimized in acetone using the Gaussian09 package,³³ with the PBE density functional.³⁴ The standard 6-31G(d)^{35,36} basis set was used for all H, C, N, F and O atoms; the Stuttgart triple zeta basis set (SDD),³⁷ along with the associated ECP to describe the 10 core electron, was employed for Cu and Fe. In addition, an extra diffuse function³⁸ was employed in the optimization of the negatively charged iron complexes. Solvation free energies are computed with the (IEF-PCM) continuum dielectric solvation model³⁹ using the radii and non-electrostatic terms for Truhlar and coworkers' SMD solvation model.⁴⁰ In all cases frequency calculations were carried out to ensure the nature of stationary points and transition states, and allowing the calculation of Gibbs free energies at 25°C and 1 atm for all the species involved in the catalytic cycles.

Additional single point calculations on the previously optimized geometries were carried out with a larger basis set. The 6-311+G** all-electron basis set³⁶ was used for all H, C, N, F and O atoms while the aug-cc-pVTZ-PP basis set including polarization and the associated electron core potential⁴¹ was employed for Cu. In the case of Fe atoms, the all-electron aug-cc-pVTZ⁴² basis set was used. The empirical dispersion terms were computed for the optimized geometries using the DFT-D3 package⁴³ by Grimme using the corresponding PBE-D⁴⁴ functional. Unless otherwise stated, all the reported energy values correspond to the Gibbs free energies obtained with the large basis sets including solvation in acetone and the dispersion corrections.

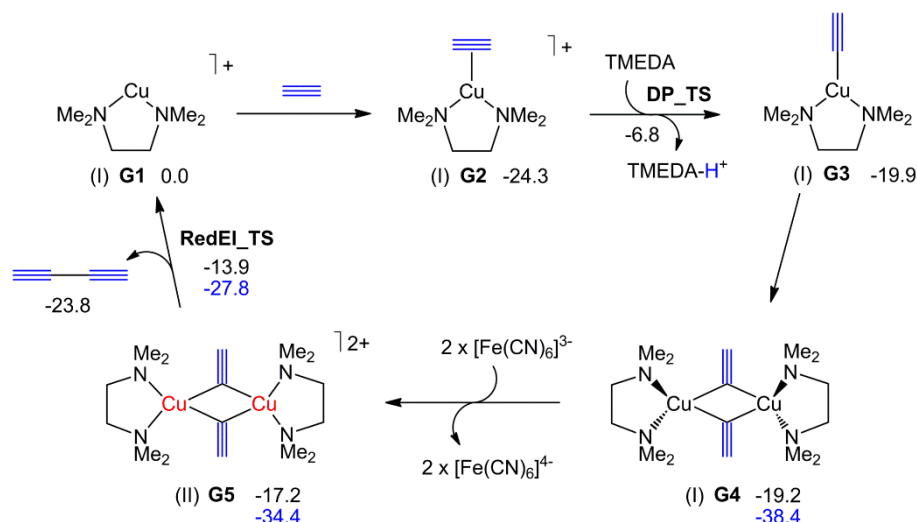
As the mechanisms involve copper (I), copper (II) and copper (III) complexes with different multiplicities, different spin states are involved. Although we computed the triplet state in a number of cases, it was always found higher in energy than the corresponding singlets, and because of that they are discussed in the text only in selected points.

Along the reaction pathways mononuclear and dinuclear species coexist, it is not easy to assign a unique origin of energies for both species at the same time. In order to get a better numeric interpretation of the catalytic cycles a colour code has been allocated to the computed free energy values; the black numbers correspond to the unique energy origin corresponding to a copper monomer, which means that the energies for the dimers have been halved. In contrast, blue numbers correspond to energies calculated in a “dinuclear” scale, where two copper monomers are considered as the origin of energies. This colour coding is useful when trying to compare energy differences along the reaction pathways; thus, when comparing a mononuclear and a dinuclear species the black number will be used whereas a comparison between two dinuclears will be computed with the blue values.

Cite this: DOI: 10.1039/c0xx00000x

www.rsc.org/xxxxxx

ARTICLE TYPE

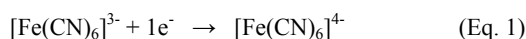


Scheme 3 Proposed mechanism for Cu(I) Glaser-Hay coupling of phenylacetylene including the computed free energy values in kcal/mol (Cu(I), Cu(II)); phenylacetylene is depicted as \equiv).

Results and Discussion

5 Outer sphere mechanisms for Glaser-Hay couplings

In this section, we describe the calculations used to explore the general mechanism for Glaser-Hay couplings where $\text{K}_3[\text{Fe}(\text{CN})_6]$ is employed as an outer sphere oxidant.⁶ Since there is no direct interaction between copper complexes and the oxidant, the latter has been treated merely as an electron source in these mechanisms; the corresponding reduction semireaction has been computed as shown in Equation 1.



First we describe the catalytic cycle for the phenylacetylene homocoupling reaction catalyzed by $[\text{Cu}(\text{TMEDA})]^+$. Additional TMEDA units are used as base, which is consistent with the excess of ligand usually introduced in the Glaser-Hay conditions. A detailed description of this catalytic cycle is shown in Scheme 3, all the species along this pathway have been named as **GX** since they are related to this general catalytic cycle. In all the schemes the copper atoms have been colour-coded to indicate the oxidation state of the metal, copper (I) is black, copper (II) is red and copper (III) is purple; additionally, in most schemes the oxidation state of the copper atom has been included between brackets. The catalytic cycle can be divided in three main steps: (i) alkyne deprotonation (from **G1** to **G3**), (ii) copper oxidation (from **G3** to **G5**), and (iii) reductive elimination (from **G5** to **G1**). The catalytic cycle starts with the π -coordination of phenylacetylene to the copper (I)-TMEDA complex (**G1**) to form the π -acetylene complex **G2**. This latter compound is more stable than the starting materials (-24.3 kcal/mol), and it seems plausible that the alkyne coordination to **G1** may be barrierless.

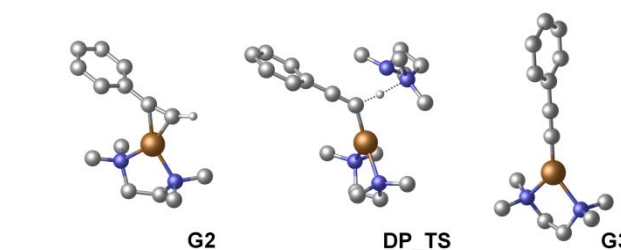


Fig. 1 Detailed structures of **G2**, **DP_TS** and **G3**.

G2 presents the expected trigonal geometry, with the metal coordinating both C_{sp} atoms. Next, the alkyne C-H terminal bond is activated by the base, a free TMEDA ligand, to yield the copper (I)- σ -acetylide complex (**G3**); this process is mediated by the corresponding transition state for the deprotonation (**DP_TS**) which lies 17.5 kcal/mol higher than **G2**. The alternative intramolecular deprotonation pathway, where TMEDA is bound to the metal before the proton transfer, has been also calculated, affording a very similar barrier (see ESI). The relative energy of **G3** is around 4 kcal/mol above than that of **G2**, indicating that the deprotonation process is slightly endergonic. Detailed structures of **G2**, **DP_TS** and **G3** are provided in Figure 1.

The dimerization of **G3** yields the corresponding copper (I) dinuclear species **G4**; in this intermediate both copper atoms adopt tetrahedral geometries, with the TMEDA ligands perpendicular to the $\text{Cu}_2\text{-C}_{(\text{sp})_2}$ planar core. This process is practically thermoneutral, as less than 2 kcal/mol are required. Dicopper (I) complex **G4** is oxidized by the iron complexes to the dicopper (II) analog **G5**, just four kcal/mol are required for this process. **G5** complex corresponds to the closed-shell singlet structure; with a bonding orbital delocalized in the two copper centers, the related triplet had a slightly higher energy. All the

attempts to locate the open-shell singlet analogue, with one

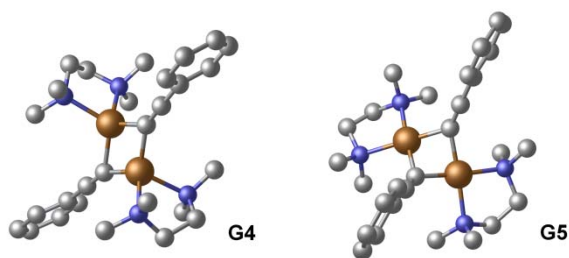


Fig. 2 Detailed structures of G4 and G5.

unpaired electron on each copper (II) center i.e. the
antiferromagnetic solution, were unsuccessful. Nevertheless it is
expected that the energy difference between these three electronic
states is small. G5 is quite symmetrical: both copper atoms adopt
almost square-planar geometries where the Cu–C_{sp} distances are
1.96 and 1.99 Å. Interestingly, the Cu₂C₂ core is not planar; the
angle between both copper planes takes a value of 127° and both
acetylide substituents lie quite close (C_{sp}–C_{sp} distance is 2.49 Å).
A detailed structural representation of intermediates G4 and G5
can be found in Figure 2. An alternative pathway associated to
the alkynyl metathesis that would yield G1 and a bisalkynyl
copper (III) complex was studied and discarded because it was
not possible to correctly optimize the latter structure.

The transition state for the bimetallic reductive elimination
(RedEI_TS) has been found to be only 6.6 kcal/mol higher than
G5, making this stage a very easy process. The geometry of this
transition state, which looks very similar to G5, shows that the
distance between the acetylide groups has been shortened to 1.88
Å. The release of the coupled diphenyldiacetylene takes the
catalytic cycle back to the starting point. The overall energetics
indicate that the reaction is exergonic by 23.8 kcal/mol. The
computed Gibbs free energies allow the calculation of the
apparent activation energy for the reaction, which can be related
to the turnover frequency. This can be easily done by means of
the energetic span model developed by Kozuch and Shaik.⁴⁵ This
methodology states that the apparent activation barrier
corresponds to the energy difference between the highest and the
lowest species when the latter appears first in the catalytic cycle,
as in our case of study. In this case the activation barrier is 17.5
kcal/mol and corresponds to the deprotonation process of the
coordinated alkyne (from G2 to DP_TS). The magnitude of this
barrier indicates that the reaction could be easily carried out at
room temperature; moreover, the barrier is independent of the
oxidant nature in agreement with the fact that any other oxidant
stronger (or even slightly weaker) than K₃[Fe(CN)₆] (+0.36 V)
can be used to carry out this reaction. Our mechanism is also
consistent with the rate acceleration by stronger bases and more
acidic alkynes, as both participate in the deprotonation step. This
was further confirmed by the additional calculations summarized
in Table 1.

In the computed catalytic cycle, all intermediates contain
copper (I), except G5, that has copper (II). G5 is generated in the
oxidation step, and yields immediately a low barrier reductive
elimination. Attempts to compute alternative catalytic cycles,
with an earlier oxidation step and more copper (II) intermediates
produced higher energy barriers. The mechanism is nevertheless

consistent with the experimental efficiency of systems where the
catalyst is introduced as a copper (II) complex (e.g. CuCl₂,

Table 1 Rate limiting step dependence on base and substrate (kcal/mol).

Base	Base Influence		Barrier
	G2	DP_TS	
NH ₃	-24.3	-1.8	22.5
TMEDA	-24.3	-6.8	17.5
OH ⁻	-24.3	-20.8	3.5
R	Substrate influence (R–PhC≡CH)		Barrier
	G2	DP_TS	
<i>p</i> -F	-24.1	-7.2	16.9
<i>p</i> -H	-24.3	-6.8	17.5
<i>p</i> -Me	-25.7	-7.3	18.4

Cu(OAc)₂ or Cu(NO₃)₂ in the reaction media.^{10,13} This requires a
simple "precatalytic" cycle where copper (II) is converted into
copper (I) by means of a preliminary alkyne homocoupling as
described in the literature.⁴⁶ This precatalytic stage, depicted in
Scheme 4, starts with the coordination of a free phenylacetylene
to G1' to yield the π-acetylene complex G2'. The deprotonation,
using a free TMEDA ligand, is an almost barrierless process
since only 0.6 kcal/mol are required. Once G3' is obtained the
copper (II) dimer G5 is formed, then the reductive elimination
takes place and the product is released, generating the copper (I)
catalyst that may continue the catalytic reaction. The computed
Gibbs free energies indicate that for this precatalytic stage the
barrier is just 6.6 kcal/mol, corresponding to the bimetallic
reductive elimination process (computed as the free energy
difference between G5 and RedEI_TS). Nevertheless, since the
catalytic reaction corresponds to the one described in Scheme 3,
the overall barrier for the whole reaction would be, as stated
above, the alkyne deprotonation (17.5 kcal/mol. Scheme 4
provides a low energy pathway to reduce Cu(II) precursors to
Cu(I) material to enter the catalytic cycle, though other
mechanisms could also be envisaged involving participation of
external base or ligand metathesis. This is in any case a side
question, as none of these steps participate in the main catalytic
cycle.

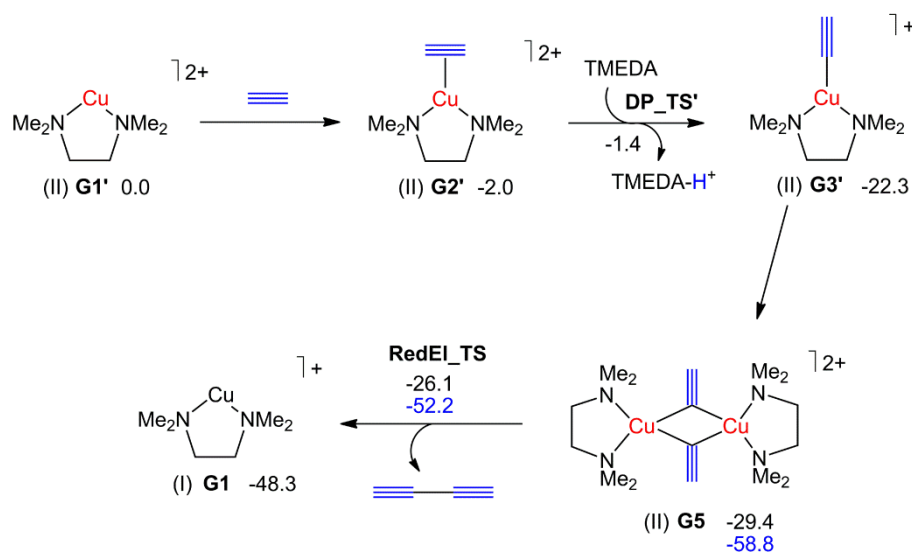
A distinct alternative would be that the process described in
Scheme 4 were the main catalytic cycle, which could then be
closed by the oxidation of G1 to G1' by the external oxidant.
This oxidation step would have a similar barrier to that of the
deprotonation in the main cycle reported above. However, we
discarded this alternative mechanism, because in this case the rate
would depend on the oxidant, and not on the nature of the base,
contrary to experimental observation.

Inner sphere mechanism for the Glaser–Hay coupling: Modeling the Cu–O₂ interactions

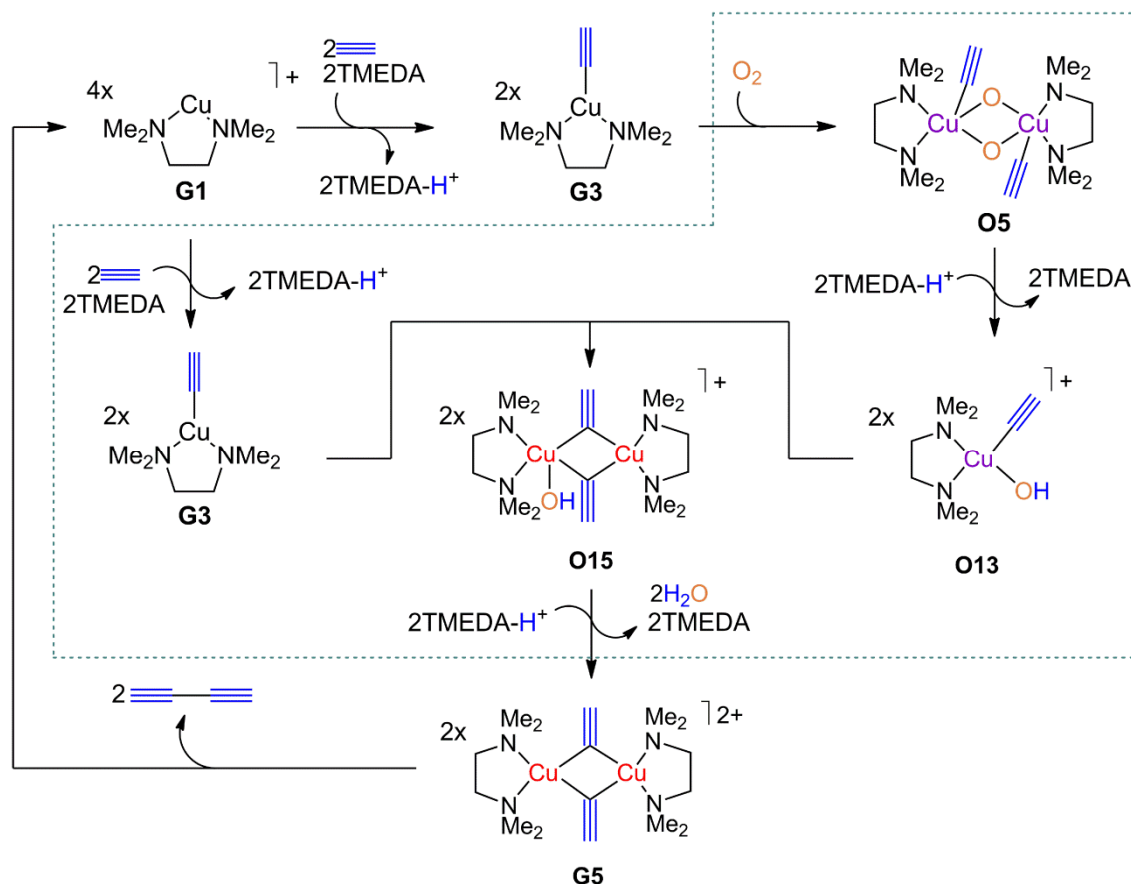
In this section the complete mechanism of the Glaser–Hay
coupling using dioxygen as oxidising agent is described.
Although O₂ and some Cu/O₂ species are recognized as good
outer sphere oxidants it should be expected that this kind of
systems reacted following an inner sphere pathway,^{27,28} in fact,
the studied Cu(I)/TMEDA/O₂ system has been reported to act as
such in C–H activation processes.⁴⁷ The explicit use of dioxygen
introduces a lot of additional steps in the catalytic cycle, and

because of this we start by presenting a simplified picture of the overall mechanism in Scheme 5, where only the most significant species are shown. The three main steps described above (Scheme 3) for the reaction with the external oxidant are conserved: (i) alkyne deprotonation (from **G1** to **G3**), (ii) copper oxidation (from **G3** to **G5**), and (iii) reductive elimination (from

G5 to **G1**). Steps (i) and (iii) are identical, and will therefore not be further discussed. However, step (ii), the copper oxidation, is much more complicated, and can be divided in three additional substeps: (iia) dioxygen cleavage (from **G3** to **O5**), (iib) first oxygen protonation (from **O5** to **O13**), (iic) second oxygen



Scheme 4 Proposed precatalytic cycle for the Cu(II)-catalyzed Glaser coupling of phenylacetylene including the computed free energy values in kcal/mol (Cu(I), Cu(II)); phenylacetylene is depicted as \equiv).



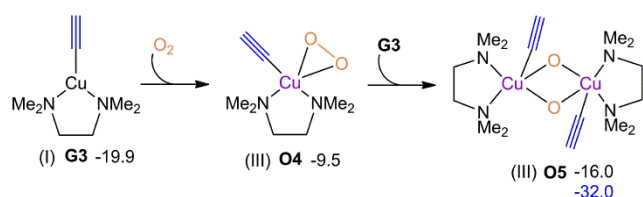
Scheme 5 Simplified mechanism for the full catalytic cycle of the Glaser Hay coupling of phenylacetylene using dioxygen as oxidant (Cu(I), Cu(II), Cu(III)); phenylacetylene is depicted as \equiv). The dotted box highlights the intermediates involved in the oxidation step.

15

Cite this: DOI: 10.1039/c0xx00000x

www.rsc.org/xxxxxx

ARTICLE TYPE



Scheme 6 Proposed mechanism for oxygen cleavage in the Glaser Hay coupling of phenylacetylene including the computed free energy values in kcal/mol (Cu(I), Cu(III)); phenylacetylene is depicted as \equiv).

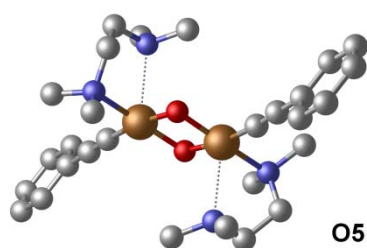


Fig. 3 Detailed structure of **O5**.

protonation and water extrusion (from **O13** to **G5**). In all cases species containing incoming oxygen atoms are noted as **OX** while species that have appeared before maintain the **GX** notation. All the free energy values presented in these schemes and subsequent tables are computed using the same energy reference (**G1**).

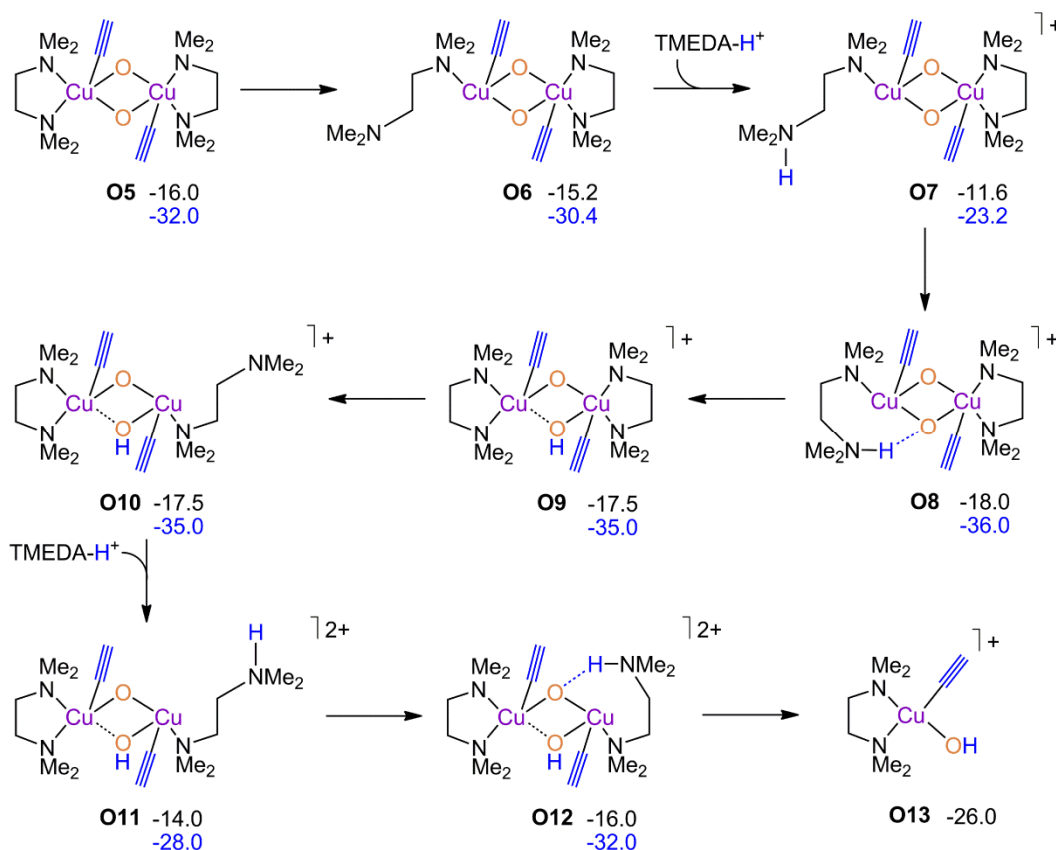
The oxygen cleavage takes part in two steps (Scheme 6). Intermediate **G3**, resulting from alkyne deprotonation, reacts with O_2 (in the triplet state) and, after a 2-electron transfer, the σ -acetylide-copper (III)- η^2 -peroxo complex **O4** is obtained. It was not possible to find any copper (I)- O_2 species, or copper (II)-superoxo complex, which may be formed prior to the electron transfer. The step from **G3** to **O4** involves a spin-crossing from triplet to singlet, likely through a low barrier minimum energy crossing point (MECP). In **O4** the copper atom adopts a slightly distorted square pyramidal structure, with the peroxo occupying two coordination sites and one nitrogen atom of the TMEDA ligand lying far in an axial position at 2.43 Å of the metal. The peroxide moiety is bound to the copper in a side-on manner, with both Cu–O distances close to 1.89 Å. This first oxidation process is endergonic, as **O4** is 10.3 kcal/mol above the previous intermediate. The coordination of a second **G3** complex to **O4**, implies the second two-electron transfer, and yields the bis(μ -oxo)-dicopper (III) complex **O5** (Figure 3) which is only 3.9 kcal/mol above **G3** (mononuclear energy scale). The relatively low free energy of **O5** is remarkable: there are several molecular units getting together to form this species, with the associated entropic penalty (see ESI). This entropic penalty is compensated in this case by a substantial enthalpic gain. The structure of **O5** shows both copper atoms adopt square pyramidal geometries with one arm of the TMEDA ligand occupying the axial position at distances longer than 2.71 Å from the metal, accordingly to the

metal center electronic configuration (d^8). As expected, the Cu_2O_2 core is planar and almost symmetrical, with a Cu–Cu distance of 2.83 Å, the Cu–O distances are close to 1.84 Å and the O–O distance is 2.37 Å; matching perfectly those measured experimentally for similar copper systems bearing nitrogen ligands.²⁸ This species is probably in equilibrium with its corresponding μ - η^2 - η^2 -peroxodicopper (II) complex; however, our calculations show that the latter lies more than 8 kcal/mol higher than **O5**. We did not locate any transition states in the potential energy surface for these bimolecular processes, but if they exist, they should be fairly low. The highest energy of this oxygen cleavage step is that of **O4**, which at -9.5 kcal/mol is well below the energy of the preceding transition step for alkyne deprotonation. After the oxygen cleavage, comes substep (iib) the first proton transfer to the oxygen. The best pathway we have found for this process is shown in Scheme 7 where the TMEDA ligands act as proton shuttles that allow the cleavage of the Cu_2O_2 core. Of course, alternative pathways are plausible, see Supporting Information, and it would not be unexpected that the reaction could proceed by one of those to give rise to the same product formation with energy requirements not very different to the ones shown here. In the pathway proposed in Scheme 7, the reaction proceeds from **O5** by the cleavage of the C–N_{axial} bond for one of the copper atoms; a step that requires less than 2 kcal/mol. Once **O6** is formed, a proton transfer between the nitrogen and one of the free protonated TMEDA ligands (obtained in the acetylene deprotonation step) happens. This process, which is endergonic by another 7.2 kcal/mol, yields the complex **O7**. Then the proton transfer occurs between the TMEDA and the oxygen atom and **O9**, with a protonated bridging oxygen, is obtained. The second bridge protonation follows the same reaction sequence until complex **O12**, with the two bridging oxygen atoms protonated. After the proton transfer to the oxygen atom the dimeric species are no longer stable and two monomeric **O13** species are formed; this copper (III) intermediate adopts the expected square planar geometry and constitutes the lowest free energy point in the catalytic cycle so far. Process (iib) involves minor energy changes in most steps, and does not change the identity of the previously determined rate-limiting steps. The metal remains as copper (III) through all these steps.

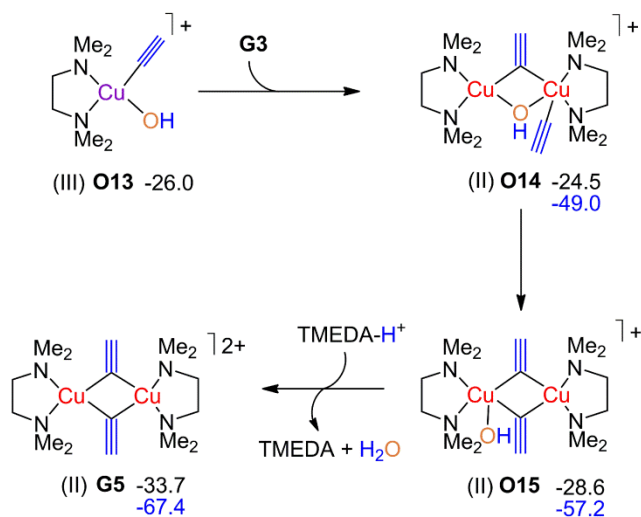
The reaction follows then the pathway shown in Scheme 8 where a water molecule is removed from the system. **O13** reacts with the copper (I) intermediate **G3** formed in the first steps of the reaction; the formation of the dimeric species **O14** involves a concomitant one-electron transfer from one copper center to the other one through the bridging alkynyl and hydroxyl groups. In this point, our mechanistic proposal diverges from that of Fomina and co-workers, as they proposed the formation of dimeric species from the equivalent of two **O13** units. This complex would be a copper(III) dimer, and have a completely different behaviour, and substantially higher energy than the copper(II) dimer we are proposing. The conversion from **O13** plus **G3** to **O14** is almost thermoneutral (only 1.5 kcal/mol are required) and

yields a structure where the bridging groups lie practically at the same distance from both copper atoms. A small rearrangement of

ligands in **O14**, where the hydroxo bridging group is replaced by the second alkyne, provides the bis- μ -alkynyl dimer **O15**.



Scheme 7 Proposed mechanism for the bis-oxo bridge protonation in the Glaser-Hay coupling of phenylacetylene including the computed free energy values in kcal/mol (Cu(III); phenylacetylene is depicted as \equiv).



Scheme 8 Proposed mechanism for the second oxygen protonation and water extrusion in the Glaser-Hay coupling of phenylacetylene including the computed free energy values in kcal/mol (Cu(II), Cu(III); phenylacetylene is depicted as \equiv).

The protonation of the hydroxyl group by TMEDA- H^+ , produces one molecule of water and the dinuclear species **G5** that is ready

for the reductive elimination step described above in the outer-sphere mechanism. This second protonation and extrusion process is a downhill sequence that does not bring any significant barrier to the overall catalytic cycle.

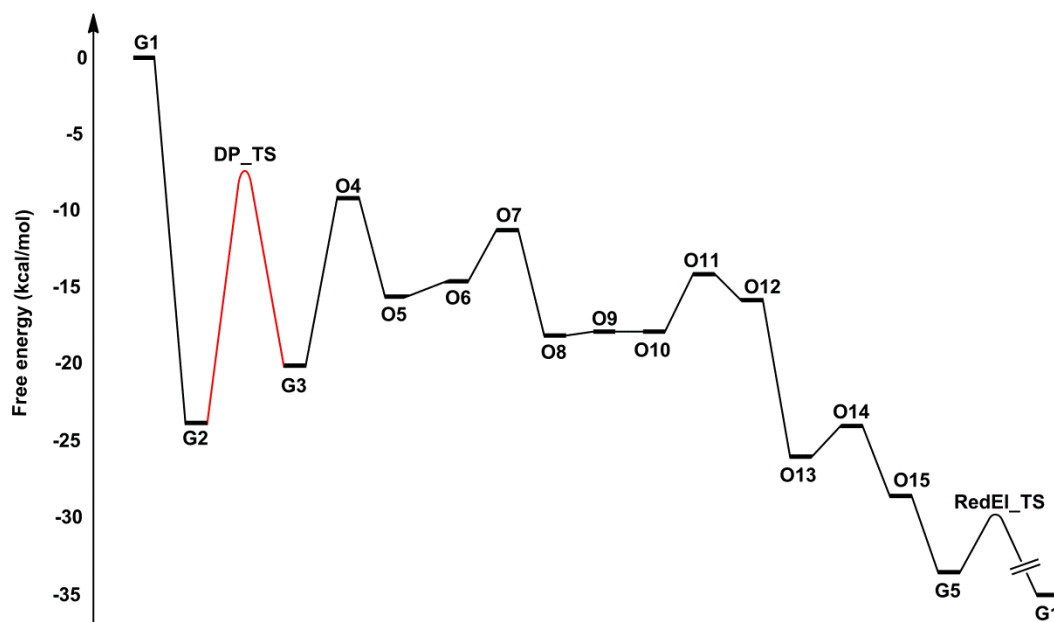
The reaction energy, computed as the formation of a diphenyldiacetylene from two phenylacetylenes and one half of dioxygen, is exergonic by 56.9 kcal/mol, in agreement with the strong oxidizing power of O_2 to H_2O . Although the mechanism for this inner sphere mechanism looks more complicated than the one for outer sphere oxidants, the apparent reaction barrier⁴⁵ remains the same (17.5 kcal/mol) corresponding to the deprotonation of the coordinated alkyne, confirming that the reaction rate is independent of the nature of the oxidant and indicating that it should work smoothly at room temperature. Scheme 9 shows the complete free energy profile of the studied reaction, with this key step, from **G2** to **DP_TS**, highlighted. It is also worth mentioning that copper (III) intermediates appear when dioxygen is applied, pointing to a more specific role for copper in this particular case.

Of course, it would be possible to think about an outer sphere mechanism involving dioxygen, where a η^1 -superoxocopper (II)

Cite this: DOI: 10.1039/c0xx00000x

www.rsc.org/xxxxxx

ARTICLE TYPE



Scheme 9 Complete free energy profile (in kcal/mol) for the Glaser-Hay reaction, the rate-limiting step is indicated in red.

or a η^2 -peroxocopper (III) could act as oxidants. This alternative pathway has also been computed and can be found in the Supporting Information. The barriers found are quite low, but still higher than those of the inner sphere mechanism here described. Moreover, an outer sphere mechanism would not comply with what is observed experimentally for similar systems i.e. whenever TMEDA is used along copper in presence of dioxygen the dinuclear bis(μ -oxo)-dicopper (III) complexes are observed.⁴⁷ This result favoring the inner sphere may seem to be in contrast with the fact that most experimental evidence on copper-dioxygen interactions focuses on the intermediates of outer sphere electron transfers.²⁶⁻²⁸ A more careful analysis of experimental literature shows however that the observation of these intermediates requires the use of specific, usually bulky ligands, in the understanding that in the absence of those an inner sphere mechanism would operate.²⁷

Conclusions

The mechanism of the Glaser-Hay oxidative coupling of terminal alkynes has been characterized by DFT means. In the case of copper (I) couplings where an outer sphere oxidant is employed, the mechanism resembles the classical Bohlmann proposal: first the alkyne coordinates to copper, enhancing the acidity of the terminal proton that can be abstracted by an external base. After deprotonation the copper (I)- σ -acetylide dimerizes and can be oxidized by most outer-sphere oxidants to yield the corresponding copper (II) dimers; finally, a fast bimetallic reductive elimination yields the product. If copper (II) is used as

starting material, there is a minor nuance in the form of low barrier precatalytic cycle where the first 1,3-diyne unit is produced, the mechanism then reverting to that for copper (I) catalysts.

In the case where dioxygen is employed as an inner-sphere oxidant, the mechanism follows a pathway similar to that of natural oxidases. Bis(μ -oxo)-dicopper (III) complexes are formed in first instance, after the protonation of the bridge a reaction between copper (I) and copper (III) yields the same copper (II) dimers as in the outer-sphere mechanism and, from those, the C_{sp} - C_{sp} coupling reaction is quite easy.

The rate-limiting step for all the studied reactions corresponds to the Cu-coordinated alkyne deprotonation, demonstrating why more acidic acetylenes and stronger bases provide higher reaction rates. In addition, the calculated barrier is low enough (17.5 kcal/mol) to allow the reaction to proceed at room temperature, as observed experimentally.

Notes and references

^a Institute of Chemical Research of Catalonia (ICIQ), Avda. Paisos Catalans 16, 43007 Tarragona, Catalonia, Spain. Fax: (+34) 977920231 E-mail: fmaseras@iciq.es

^b Henkel AG & Co. KGaA, Henkelstrasse 67, 40589 Düsseldorf, Germany.

^c Departament de Química, Universitat Autònoma de Barcelona, 08193, Barcelona, Spain.

† Electronic Supplementary Information (ESI) available: Includes all computed potential energies, enthalpies, free energies, dispersion corrections, energy profiles and optimized structures, along alternative Glaser-Hay pathways. See DOI: 10.1039/b000000x/

1. R. Bates, *Organic Synthesis using Transition Metals*, Wiley-Blackwell, Sheffield, UK, 2000; J. F. Hartwig, *Organotransition Metal Chemistry: From Bonding to Catalysis*, University Science Books, U.S., Sausalito, US, 2009.
2. The Nobel Prize in Chemistry 2010 - Richard F. Heck, Ei-ichi Negishi, Akira Suzuki Nobelprize.org. 6 June 2010. http://nobelprize.org/nobel_prizes/chemistry/laureates/2010/
3. T. Hamada, X. Ye and S. S. Stahl, *J. Am. Chem. Soc.*, 2008, **130**, 833; W. Yin, C. He, M. Chen, H. Zhang and A. Lei, *Org. Lett.*, 2008, **11**, 709; X. Guo, R. Yu, H. Li and Z. Li, *J. Am. Chem. Soc.*, 2009, **131**, 17387; R. J. Lundgren and M. Stradiotto, *Angew. Chem. Int. Ed.*, 2010, **49**, 9322.
4. P. Tundo, P. A. D. a. S. Black, J. Breen, T. Collins, S. Memoli, J. Miyamoto, M. Polyakoff and W. Tumas, *Pure Appl. Chem.*, 2000, **72**, 12007.
5. C. Glaser, *Ber. Dtsch. Chem. Ges.*, 1869, **2**, 422; C. Glaser, *Justus Liebigs Ann. Chem.*, 1870, **154**, 137.
6. A. Baeyer and L. Landsberg, *Ber. Dtsch. Chem. Ges.*, 1882, **15**, 57; F. J. Brockman, *Can. J. Chem.*, 1955, **33**, 507.
7. A. Vaitiekunas and F. F. Nord, *J. Am. Chem. Soc.*, 1954, **76**, 2733; Y. Odaira, *Bull. Chem. Soc. Jpn.*, 1956, **29**, 470; P. Siemsen, R. C. Livingston and F. Diederich, *Angew. Chem. Int. Ed.*, 2000, **39**, 2632; J. J. Li, *Name Reactions for Homologation, Part 1*, John Wiley & Sons Inc., Hoboken, New Jersey, 2009.
8. A. Hay, *J. Org. Chem.*, 1960, **25**, 1275; A. S. Hay, *J. Org. Chem.*, 1962, **27**, 3320.
9. E. Valentí, M. A. Pericàs and F. Serratos, *J. Am. Chem. Soc.*, 1990, **112**, 7405; N. Hebert, A. Beck, R. B. Lennox and G. Just, *J. Org. Chem.*, 1992, **57**, 1777; E. W. Kwock, T. Baird and T. M. Miller, *Macromolecules*, 1993, **26**, 2935; F. M. Menger, X. Y. Chen, S. Brocchini, H. P. Hopkins and D. Hamilton, *J. Am. Chem. Soc.*, 1993, **115**, 6600; D. W. J. McCallien and J. K. M. Sanders, *J. Am. Chem. Soc.*, 1995, **117**, 6611; S. Hoger, A.-D. Meckenstock and H. Pellen, *J. Org. Chem.*, 1997, **62**, 4556; R. E. Martin, T. Mäder and F. Diederich, *Angew. Chem. Int. Ed.*, 1999, **38**, 817; M. A. Heuft, S. K. Collins, G. P. A. Yap and A. G. Fallis, *Org. Lett.*, 2001, **3**, 2883; K. Miyawaki, R. Goto, T. Takagi and M. Shibakami, *Synlett*, 2002, 1467; X. Xie, P.-W. Phuan and M. C. Kozlowski, *Angew. Chem. Int. Ed.*, 2003, **42**, 2168; Q. Zheng and J. A. Gladysz, *J. Am. Chem. Soc.*, 2005, **127**, 10508; L. Chu and F.-L. Qing, *J. Am. Chem. Soc.*, 2010, **132**, 7262; X. Jia, K. Yin, C. Li, J. Li and H. Bian, *Green Chem.*, 2011, **13**, 2175; K. Yin, C. Li, J. Li and X. Jia, *Green Chem.*, 2011, **13**, 591; S. Zhang, X. Liu and T. Wang, *Adv. Synth. Catal.*, 2011, **353**, 1463. S. E. Allen, R. R. Walvoord, R. Padilla-Salinas and M. C. Kozlowski, *Chem. Rev.*, 2013, **113**, 6234.
10. J. J. Pak, T. J. R. Weakley and M. M. Haley, *J. Am. Chem. Soc.*, 1999, **121**, 8182.
11. L. Li, J. Wang, G. Zhang and Q. Liu, *Tetrahedron Lett.*, 2009, **50**, 4033.
12. Q. Zheng, R. Hua and Y. Wan, *Appl. Organometal. Chem.*, 2010, **24**, 314.
13. H. A. Stefani, A. S. Guarezemini and R. Cella, *Tetrahedron*, 2010, **66**, 7871.
14. D. Li, K. Yin, J. Li and X. Jia, *Tetrahedron Lett.*, 2008, **49**, 5918.
15. K. Yin, C.-J. Li, J. Li and X.-S. Jia, *Appl. Organometal. Chem.*, 2011, **25**, 16.
16. F. Bohlmann, H. Schönowsky, E. Inhoffen and G. Grau, *Chem. Ber.*, 1964, **97**, 794.
17. M. B. Nielsen and F. Diederich, *Chem. Rev.*, 2005, **105**, 1837.
18. A. Stütz, *Angew. Chem. Int. Ed.*, 1987, **26**, 320.
19. P. J. Stang and F. Diederich, *Modern Acetylene Chemistry*, Weinheim, 1995; J. M. Tour, *Chem. Rev.*, 1996, **96**, 537.
20. A. E. Wendlandt, A. M. Suess and S. S. Stahl, *Angew. Chem. Int. Ed.*, 2011, **50**, 11062; A. N. Campbell and S. S. Stahl, *Acc. Chem. Res.*, 2012, **45**, 851.
21. Q. Liu, P. Wu, Y. Yang, Z. Zeng, J. Liu, H. Yi and A. Lei, *Angew. Chem. Int. Ed.*, 2012, **51**, 4666; Y.-F. Wang, H. Chen, X. Zhu and S. Chiba, *J. Am. Chem. Soc.*, 2012, **134**, 11980.
22. C. Sens, I. Romero, M. Rodríguez, A. Llobet, T. Parella and J. Benet-Buchholz, *J. Am. Chem. Soc.*, 2004, **126**, 7798; L. Duan, F. Bozoglian, S. Mandal, B. Stewart, T. Privalov, A. Llobet and L. Sun, *Nature Chem.*, 2012, **4**, 418; M. L. Rigby, S. Mandal, W. Nam, L. C. Spencer, A. Llobet and S. S. Stahl, *Chem. Sci.*, 2012, **3**, 3058.
23. L. Fomina, B. Vazquez, E. Tkatchouk and S. Fomine, *Tetrahedron*, 2002, **58**, 6741.
24. C. J. Cramer, A. Kinal, M. Włoch, P. Piecuch and L. Gagliardi, *J. Phys. Chem. A*, 2006, **110**, 11557; C. J. Cramer, M. Włoch, P. Piecuch, C. Puzzarini and L. Gagliardi, *J. Phys. Chem. A*, 2006, **110**, 1991.
25. B. F. Gherman and C. J. Cramer, *Coord. Chem. Rev.*, 2009, **253**, 723.
26. A. P. Cole, D. E. Root, P. Mukherjee, E. I. Solomon and T. D. P. Stack, *Science*, 1996, **273**, 1848; E. I. Solomon, U. M. Sundaram and T. E. Machonkin, *Chem. Rev.*, 1996, **96**, 2563; L. Q. Hatcher and K. D. Karlin, *J. Biol. Inorg. Chem.*, 2004, **9**, 669.
27. E. A. Lewis and W. B. Tolman, *Chem. Rev.*, 2004, **104**, 1047.
28. L. M. Mirica, X. Ottenwaelder and T. D. P. Stack, *Chem. Rev.*, 2004, **104**, 1013.
29. P. Kang, E. Bobyr, J. Dustman, K. O. Hodgson, B. Hedman, E. I. Solomon and T. D. P. Stack, *Inorg. Chem.*, 2010, **49**, 11030; Y. Gao, G. Wang, L. Chen, P. Xu, Y. Zhao, Y. Zhou and L.-B. Han, *J. Am. Chem. Soc.*, 2009, **131**, 7956; H. Rao, H. Fu, Y. Jiang and Y. Zhao, *Adv. Synth. Catal.*, 2010, **352**, 458; J.-S. Tian and T.-P. Loh, *Angew. Chem. Int. Ed.*, 2010, **49**, 8417; Y. Wei, H. Zhao, J. Kan, W. Su and M. Hong, *J. Am. Chem. Soc.*, 2010, **132**, 2522; C. Zhang and N. Jiao, *Angew. Chem. Int. Ed.*, 2010, **49**, 6174.
30. N. Hewitt and A. Rauk, *J. Phys. Chem. B*, 2009, **113**, 1202; J. Jover and F. Maseras, *Chem. Commun.*, 2013, **49**, 10486.
31. M. García-Melchor, A. A. C. Braga, A. Lledós, G. Ujaque and F. Maseras, *Acc. Chem. Res.*, 2013, **46**, 2626; A. A. C. Braga, N. H. Morgon, G. Ujaque and F. Maseras, *J. Am. Chem. Soc.*, 2005, **127**, 9298; A. Nova, G. Ujaque, F. Maseras, A. Lledós and P. Espinet, *J. Am. Chem. Soc.*, 2006, **128**, 14571; B. Fuentes, M. García-Melchor, A. Lledós, F. Maseras, J. A. Casares, G. Ujaque and P. Espinet, *Chem. Eur. J.*, 2010, **16**, 8596; C. Mollar, M. Besora, F. Maseras, G. Asensio and M. Medio-Simón, *Chem. Eur. J.*, 2010, **16**, 13390.
32. G. J. Christian, A. Llobet and F. Maseras, *Inorg. Chem.*, 2010, **49**, 5977; A. Conde, L. Vilella, D. Balcells, M. M. Díaz-Requejo, A. Lledós and P. J. Pérez, *J. Am. Chem. Soc.*, 2013, **135**, 3887.
33. M. J. Frisch, G. W. Trucks, H. B. Schlegel, G. E. Scuseria, M. A. Robb, J. R. Cheeseman, G. Scalmani, V. Barone, B. Mennucci, G. A. Petersson, H. Nakatsuji, M. Caricato, X. Li, H. P. Hratchian, A. F. Izmaylov, J. Bloino, G. Zheng, J. L. Sonnenberg, M. Hada, M. Ehara,

- K. Toyota, R. Fukuda, J. Hasegawa, M. Ishida, T. Nakajima, Y. Honda, O. Kitao, H. Nakai, T. Vreven, J. Montgomery, J. A., J. E. Peralta, F. Ogliaro, M. Bearpark, J. J. Heyd, E. Brothers, K. N. Kudin, V. N. Staroverov, R. Kobayashi, J. Normand, K. Raghavachari, A. Rendell, J. C. Burant, S. S. Iyengar, J. Tomasi, M. Cossi, N. Rega, N. J. Millam, M. Klene, J. E. Knox, J. B. Cross, V. Bakken, C. Adamo, J. Jaramillo, R. Gomperts, R. E. Stratmann, O. Yazyev, A. J. Austin, R. Cammi, C. Pomelli, J. W. Ochterski, R. L. Martin, K. Morokuma, V. G. Zakrzewski, G. A. Voth, P. Salvador, J. J. Dannenberg, S. Dapprich, A. D. Daniels, Ö. Farkas, J. B. Foresman, J. V. Ortiz and J. F. Cioslowski, D. J. , *Gaussian09, Revision A.02*, (2009) Gaussian, Inc., Wallingford CT.
34. J. P. Perdew, K. Burke and M. Ernzerhof, *Phys. Rev. Lett.*, 1996, **77**, 3865; J. P. Perdew, K. Burke and M. Ernzerhof, *Phys. Rev. Lett.*, 1997, **78**, 1396.
35. P. C. Hariharan and J. A. Pople, *Theor. Chem. Acc.*, 1973, **28**, 213.
36. M. J. Frisch, J. A. Pople and J. S. Binkley, *J. Chem. Phys.*, 1984, **80**, 3265.
37. T. H. Dunning and P. J. Hay, in *Modern Theoretical Chemistry*, ed. H. F. Schaefer III, Plenum, New York, 1976, vol. 3, pp. 1; A. Bergner, M. Dolg, W. Küchle, H. Stoll and H. Preuss, *Molecular Physics*, 1993, **80**, 1431
38. T. Clark, J. Chandrasekhar, G. W. Spitznagel and P. V. R. Schleyer, *J. Comput. Chem.*, 1983, **4**, 294.
39. D. J. Tannor, B. Marten, R. Murphy, R. A. Friesner, D. Sitkoff, A. Nicholls, B. Honig, M. Ringnalda and W. A. Goddard, *J. Am. Chem. Soc.*, 1994, **116**, 11875; B. Marten, K. Kim, C. Cortis, R. A. Friesner, R. B. Murphy, M. N. Ringnalda, D. Sitkoff and B. Honig, *J. Phys. Chem.*, 1996, **100**, 11775.
40. A. V. Marenich, C. J. Cramer and D. G. Truhlar, *J. Phys. Chem. B*, 2009, **113**, 6378.
41. K. A. Peterson and C. Puzzarini, *Theor. Chem. Acc.*, 2005, **114**, 283.
42. N. B. Balabanov and K. A. Peterson, *J. Chem. Phys.*, 2005, **123**, 064107.
43. *DFT-D3 A dispersion correction for density functionals, Hartree-Fock and semi-empirical quantum chemical methods*, (2011) Universität Bonn.
44. S. Grimme, *J. Comput. Chem.*, 2004, **25**, 1463; S. Grimme, *J. Comput. Chem.*, 2006, **27**, 1787; S. Grimme, *J. Chem. Phys.*, 2010, **132**, 154104.
45. S. Kozuch and S. Shaik, *Acc. Chem. Res.*, 2010, **44**, 101.
46. W. S. Brotherton, H. A. Michaels, J. T. Simmons, R. J. Clark, N. S. Dalal and L. Zhu, *Org. Lett.*, 2009, **11**, 4954; G. Zhang, H. Yi, G. Zhang, Y. Deng, R. Bai, H. Zhang, J. T. Miller, A. J. Kropf, E. E. Bunel and A. Lei, 2014, **136**, 924.
47. P. Kang, E. Bobyr, J. Dustman, K. O. Hodgson, B. Hedman, E. I. Solomon and T. D. P. Stack, *Inorg. Chem.*, 2010, **49**, 11030.